Ultrafast Spectroscopic Investigation of the Charge Recombination Dynamics of Ion Pairs Formed upon Highly Exergonic Bimolecular Electron-Transfer Quenching: Looking for the Normal Region

Stéphane Pagès, Bernhard Lang, and Eric Vauthey*

Department of Physical Chemistry, University of Geneva, 30 quai Ernest Ansermet, CH-1211 Geneva 4, Switzerland

Received: September 18, 2003; In Final Form: November 18, 2003

The charge recombination dynamics of the ion pairs formed upon electron-transfer quenching of perylene by tetracyanoethylene in acetonitrile has been investigated using ultrafast fluorescence upconversion, transient absorption, and transient grating techniques. For this donor/acceptor pair, charge separation is highly exergonic ($\Delta G_{CS} = -2.2$ eV), but charge recombination is weakly exergonic ($\Delta G_{CR} = -0.6$ eV). It was found that for more than 90% of the ion pair population, charge recombination is ultrafast and occurs in less than 10 ps. This decay component could not be observed in a previous investigation with a lower time resolution. The results indicate that the primary quenching product is a contact ion pair and not a solvent-separated ion pair as generally assumed for highly exergonic electron-transfer quenching processes. A possible explanation for this apparent divergence is that the contact ion pair is initially formed in an electronic excited state. Only a very minor fraction of the ion pair population undergoes the slow charge recombination predicted by Marcus theory for weakly exergonic charge-transfer processes (normal region).

Introduction

Since the pioneering work of Weller and co-workers,[1] it is well known that the overall reaction scheme for the intermolecular electron transfer (ET) quenching of an excited molecule M* by a quencher Q in polar solvents involves two charge-transfer processes:

(1) A charge separation (CS) that leads, after the diffusion of the reactants to a distance where ET is operative, to the primary product, a geminate ion pair (GIP), $M^* + Q \rightarrow M^*Q \rightarrow M^{-/+}Q^{+/-}$.

(2) A charge recombination (CR) of the GIP to the neutral ground-state $M^{-/+}Q^{+/-} \rightarrow M\ Q$, which competes with its dissociation to free ions, $M^{-/+}Q^{+/-} \rightarrow M^{-/+} + Q^{+/-}$.

Many studies have shown that the driving force dependencies of bimolecular CS and CR differ drastically, especially in the high-exergonicity regime:

(1) The rate constant of charge separation, k_{CS}, increases with increasing driving force, and at rather weak exergonicity (ΔG_{CS} < ca. −0.3 eV), it becomes larger than the diffusion rate constant, even in nonviscous solvents. This behavior continues up to high exergonicity (ΔG_{CS} < 2.5 eV), and the inverted region predicted by Marcus theory[2] is not observed. Several hypotheses have been proposed to account for this discrepancy, such as the formation of the product in an electronic excited state[3] and the quenching distance increasing with driving force.[4] Indeed, according to the Marcus expression for solvent reorganization energy, a larger distance implies a larger solvent reorganization energy and thus a shift of the occurrence of the inverted regime to larger driving forces. Accordingly, quenching distances as large as 12−14 Å have been invoked for highly exergonic CS processes in liquids.[5,6]

(2) In most cases, CR is highly to moderately exergonic, and the inverted region is clearly observed (i.e., k_{CR} decreases with increasing driving force[7−9]). Direct measurements of the GIP population dynamics have shown that the rate constant of CR decreases by more than 3 orders of magnitude by increasing the driving force, ΔG_{CR}, from about −1 to −3 eV.[10]

The driving-force dependence of CR in the low-exergonicity regime, $\Delta G_{CR} > -1$ eV, is not so well documented. According to Mataga and co-workers, it depends strongly on the mode of production of the GIP.[11] For GIPs generated by direct excitation in the charge-transfer band of the corresponding donor/acceptor complexes, k_{CR} continues to increase with decreasing driving force as in the higher exergonicity regime. This trend has been reported down to −0.6 eV. Thus, the so-called normal region predicted by Marcus theory (i.e., the increase of the ET rate constant with increasing driving force) is not observed. However, k_{CR} in GIPs formed by bimolecular CS exhibits the opposite dependence (i.e., it follows the normal regime of Marcus theory[12,13]).

These two different behaviors have been explained by two different types of ion pairs.[11] Pairs formed by direct charge-transfer excitation are generally called contact ion pairs (CIPs) because they are supposed to have essentially the same sandwich-type structure as the ground-state complex, with an interionic distance on the order of 3.5 Å. This is supported by the observation of charge-transfer fluorescence for the longer-lived CIPs, indicating a substantial orbital overlap of the ions, hence close contact.[14]

However, pairs formed upon ET quenching in polar solvents are generally called loose ion pairs (LIPs) or solvent-separated ion pairs (SSIPs). Because these ion pairs are formed in a highly exergonic quenching process, their interionic distance should be, according to the above-mentioned hypothesis of the driving-force-dependent quenching distance, larger than 10 Å.[5,6]

There is to our knowledge only a *single* direct observation of the normal region for the CR of ion pairs formed upon bimolecular photoinduced CS in polar solvents. It has been

* Corresponding author. E-mail: eric.vauthey@chiphy.unige.ch.

10.1021/jp036796g CCC: $27.50 © 2004 American Chemical Society
Published on Web 12/30/2003

reported for GIPs generated upon quenching of aromatic hydrocarbons in the S_1 state, such as perylene (Pe), by tetracyanothylene (TCNE) in acetonitrile.[12,13] The CR time constants were obtained from the decay of the ion population measured by transient absorption with a time resolution of about 30−50 ps. For the $Pe^{\bullet+}/TCNE^{\bullet-}$ pair, for which $\Delta G_{CR} = -0.6$ eV, a CR time constant of 1.6 ns was reported. For a more exergonic CR, namely, $\Delta G_{CR} < -1$ eV, time constants smaller than 25 ps were measured.[7] This is an apparently clear evidence of the normal region. Interestingly, when formed upon charge-transfer excitation, CR of the $Pe^{\bullet+}/TCNE^{\bullet-}$ pair is ultrafast and occurs with a time constant of 300 fs.[15]

Several attempts by our group to observe the normal region for CR were unsuccessful. In an investigation of the CR dynamics of GIPs formed upon ET quenching at high donor concentration, the normal region could not be observed even for driving forces as small as −0.6 eV.[10] Instead, CR was found to be ultrafast, and CR time constants as small as 1.8 ps were measured. Similarly, the decay of GIPs formed upon ET quenching of Zn-tetraphenylporphyrine (ZnTPP) in the S_2 state by a weak quencher, Q, occurs predominantly by CR to ZnTPP*(S_1) + Q. In this case, CR is weakly exergonic, $\Delta G_{CR} > -0.5$ eV, but takes place in less than 500 fs![16] Finally, the ion pairs formed by ET quenching of cyanoanthracene derivatives by iodoanisole undergo heavy-atom-induced triplet CR in less than 10 ps, although the driving force is on the order of −0.5 eV.[17] All of these investigations indicate that the GIPs behave more like CIPs than like LIPs and that the distinction between CIPs and LIPs according to the mode of formation, namely, charge-transfer excitation or bimolecular CS, might not be adequate.

To detect ultrafast CR components that might have been missed in the original study described above,[12] we have undertaken a reinvestigation of the CR dynamics of the $Pe^{\bullet+}/TCNE^{\bullet-}$ pair formed upon ET quenching in acetonitrile using ultrafast time-resolved spectroscopy. This ion pair is formed upon highly exergonic CS ($\Delta G_{CS} = -2.2$ eV), and CR is therefore weakly exergonic ($\Delta G_{CR} = -0.6$ eV). As shown below, this reinvestigation has revealed that most of the CR dynamics occurs on a much faster time scale than previously reported and that the normal regime predicted by Marcus theory cannot be considered to be a general behavior for CR of ion pairs formed by bimolecular CS.

Experimental Section

Ultrafast Spectroscopy. The fluorescence upconversion setup has already been described in ref 16. Excitation was achieved at 400 nm using the frequency-doubled output of a Kerr lens mode-locked Ti:sapphire laser (Tsunami, Spectra-Physics). The full width at half-maximum of the instrument response function was 210 fs.

The multiplex transient grating (TG) setup has been described in detail elsewhere.[10,18] Excitation was performed at 400 nm with the frequency-doubled output of a standard 1-kHz amplified Ti:sapphire system (Spitfire, Spectra-Physics). The duration of the pulses at 400 nm was around 100 fs. All transient grating spectra were corrected for the chirp of the probe pulse.

For transient absorption (TA) measurements, excitation was achieved at 400 nm with the same source as in the transient grating experiments. For probing, a home-built optical parametrical amplifier in noncollinear configuration, generating ultrashort pulses tunable between 480 and 700 nm, was used. For the experiment reported here, the probe wavelength was centered at 535 nm. The width of the probe-pulse spectrum was about 40 nm fwhm, well covering the D_0-D_5 absorption band of the perylene cation. The transmitted probe light was detected with a photodiode. To achieve good sensitivity, the pump light was chopped at half of the amplifier frequency, and the transmitted probe-pulse intensity was recorded shot by shot and was corrected for intensity fluctuations using a reference signal picked up in front of the sample cell. This results in a resolution on relative transmission change of less than 10^{-4} under good conditions. The full width at half-maximum cross-correlation function was around 200 fs. In all three experiments, detection was achieved at the magic angle.

Phoconductivity. The free-ion yields have been determined using photoconductivity.[19] The photocurrent cell has been described in detail previously.[20] Excitation was performed with 25-ps pulses at 355 nm generated by frequency tripling the output of an active/passive mode-locked Q-switched Nd:YAG laser (Continuum PY-61-10). The system benzophenone with 0.02 M 1,4-diazabicyclo[2,2,2]-octane in acetonitrile, which has a free-ion yield of unity, was used as a standard.[21]

Samples. Perylene (Pe) was recrystallized from benzene before use. Tetracyanoethylene (TCNE) was recrystallized from chlorobenzene and sublimed twice. Acetonitrile (ACN, UV grade) was used as received. All chemicals were from Fluka.

For fluorescence upconversion, the sample solutions were placed in a spinning cell with an optical path length of 0.4 mm. The absorbance of the samples at 400 nm was around 0.1. For transient absorption and transient grating measurements, a 1-mm-thick spinning cell was used. The absorbance at 400 nm was around 1. For photoconductivity measurements, the absorbance of the sample at 355 nm on 1 cm was around 0.5. All sample solutions were bubbled with Ar for 15−20 min before use.

Data Analysis. The fluorescence and transient absorption time profiles were analyzed by the iterative reconvolution of the instrument response function with trial functions (sum of exponentials) using a nonlinear least-squares fitting procedure (MATLAB, The MathWorks, Inc.).

Results

Pe Fluorescence Dynamics. Figure 1A shows the time profiles of Pe fluorescence measured at 495 nm with various concentrations of TCNE in ACN. At this wavelength, the fluorescence decay of Pe without TCNE is monoexponential with a time constant τ_0 on the order of 4.5 ns, depending on the degree of deoxygenation. As reported in refs 22 and 23, the fluorescence dynamics of Pe upon 400-nm excitation is wavelength-dependent during the first 10 ps because of vibrational relaxation. However, the effect of this process on the fluorescence decay at 495 nm is negligible.

Additionally, a weak but distinct oscillation of the fluorescence intensity due to the propagation of a vibrational wave packet can be observed on a short time scale (Figure 1B**)**. The frequency of this mode is around 70 cm^{-1}, rather close to the 110-cm^{-1} Raman band reported in crystalline Pe.[24]

The addition of TCNE leads to a strong acceleration of the fluorescence decay. Moreover, the fluorescence time profile is no longer monoexponential as shown in Figure 1A. At the smallest TCNE concentration used (0.02 M), a biexponential function can be reasonably well fit to the fluorescence decay. At higher TCNE concentrations, it cannot be reproduced with less than three exponential functions. The corresponding time constants and amplitudes are listed in Table 1. A plot of the ratio τ_0/τ_1 as a function of TCNE concentration is linear up to 0.32 M with a slope of 2.4×10^{10} M^{-1} s^{-1}. This value agrees

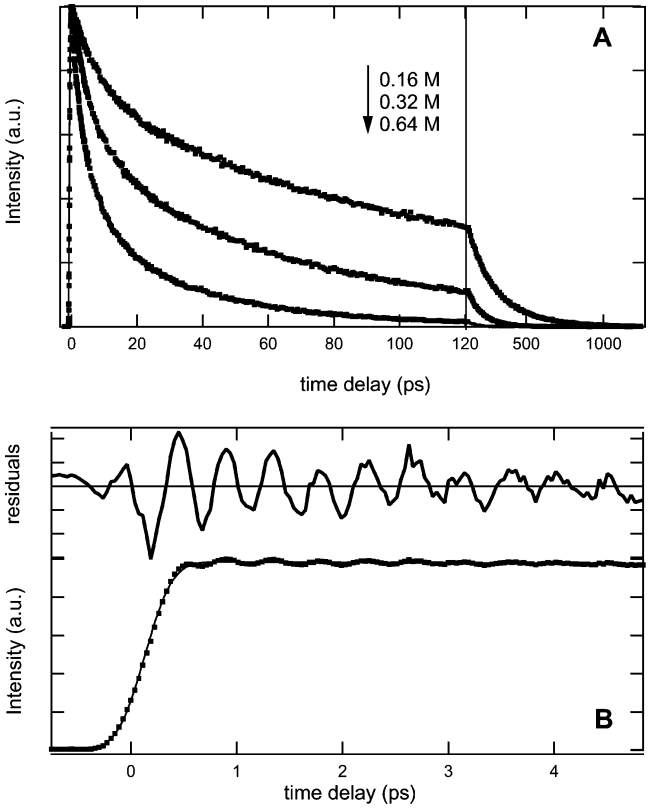

Figure 1. (A) Time profiles of the fluorescence intensity of Pe at 495 nm with various concentrations of TCNE (dots) and best fits with a triexponential function (solid line). (B) Early fluorescence dynamics of Pe in ACN without quencher (dots), best single-exponential fit (solid line), and residuals showing the motion of a vibrational wave packet.

TABLE 1: Parameters Obtained from the Triexponential Fit of the Fluorescence Time Profiles of Pe with Various TCNE Molar Concentrations in ACN

[TCNE]	τ_1 (ps)	A_1	τ_2 (ps)	A_2	τ_3 (ps)	A_3
0.02	1910	0.96	112	0.04		
0.08	395	0.7	98	0.18	13	0.12
0.16	227	0.46	94	0.29	10.6	0.25
0.32	110	0.35	31	0.35	4.0	0.3
0.64	47	0.23	13.5	0.33	2.9	0.44
0.90	20	0.18	3.67	0.74	0.330	0.08

well with the rate constant of diffusion in ACN. The faster decay components can be safely attributed to the so-called transient effect.[25] Indeed, at a given TCNE concentration, there is always an excited-state subpopulation with a quencher molecule at a distance where ET can occur without significant diffusion. A more detailed analysis of these fluorescence decays will be presented in a separate paper. However, the results listed in Table 1 are sufficient for the purpose of the present investigation.

A small decrease of the initial fluorescence intensity upon the addition of TCNE cannot be excluded. However, if present, this decrease can be estimated from our data to be less than 30% even at the largest TCNE concentration. Its origin could be due either to quenching components faster than the time resolution of the upconversion setup or to the excitation of a ground-state complex. At high TCNE concentration, a charge-transfer band can be observed in the absorption spectrum around 800 nm (i.e., very far from the excitation wavelength). This indicates that for TCNE concentrations of up to 0.9 M at least more than 70% of the absorbed photons lead to the population of the S_1 local excited state of Pe.

Ion Pair Population Dynamics. Figure 2 shows transient grating (TG) spectra measured at several time delays after excitation at 400 nm of a Pe + 0.9 M TCNE solution. As explained in detail elsewhere,[26,27] such TG spectra are very similar to transient absorption (TA) spectra, the main difference being that the TG intensity is proportional to the square of the absorption changes. The advantage of this technique over TA is its superior sensitivity because of the zero-background nature of the signal.

At short time delays, the TG spectrum is dominated by a band centered at 700 nm, which can be assigned to Pe in the S_1 state. A much weaker band due to $Pe^{\bullet +}$ [28] can also be observed at about 535 nm. After 100 ps, only this Pe cation band remains visible. These spectra compare very well with the TA spectra reported by Mataga and co-workers.[7] The TCNE radical anion exhibits a weak absorption band at 420 nm[28] and cannot be observed here.

The major drawback of TG, when population dynamics is investigated, is its sensitivity to changes in the refractive index.[29] Because of this, the TG intensity at very short time is dominated by the optical Kerr effect from the solvent, and the determination of the population dynamics during the first few hundreds of femtoseconds is problematic.[10] To avoid this problem, the population dynamics of $Pe^{\bullet +}$ was measured by performing TA measurements at 535 nm.

Figure 3 shows the time profiles of the TA at 535 nm after 400-nm excitation of solutions of Pe with various concentrations of TCNE. At the concentrations investigated here, all of the time profiles exhibit an initial prompt rise within the instrument response function, followed by a slower rise and by a decay to a plateau whose height remains constant up to 3 ns. At 0.16 M TCNE, the prompt rise is mainly due to Pe* in the S_1 state, which absorbs weakly at this wavelength. Because the initial fluorescence intensity is essentially the same at higher TCNE concentrations, the contribution of the S_1 population to the initial TA intensity at 535 nm can be expected to be the same at all TCNE concentrations. Therefore, because the time dependence of this population is known from the fluorescence measurements (see Table 1), its contribution to the TA time profile, $I_{TA}^{S1}(t)$, can be easily evaluated.

The TA time profiles, $I_{TA}^{535}(t)$, could be satisfactorily reproduced by a multiexponential function of the following form with $n = 3$:

$$I_{TA}^{535}(t) = I_{TA}^{S1}(t) + I_{TA}^{ion}(t) \qquad \text{with}$$

$$I_{TA}^{ion}(t) = A_0 + \sum_{i=1}^{n} A_i \exp\left(-\frac{t}{\tau_i}\right) \quad (1)$$

The parameters obtained from the fit of this function to the transient absorption data are listed in Table 2. The following features can be observed:

(1) The height of the plateau, A_0, decreases with increasing TCNE concentration. This plateau corresponds to the free-ion population, which decays to the neutral ground state on the microsecond time scale by homogeneous recombination.

(2) A fast rising component with a time constant on the order of 1−2 ps can be observed at each concentration. At 0.16 M TCNE, an additional slower-rising component is also present. These rises can apparently be ascribed to the formation of the ion pair.

(3) The decay depends strongly on the TCNE concentration. At high concentration, it is biphasic with an ultrafast sub-10-ps component and a slower component. At lower concentration,

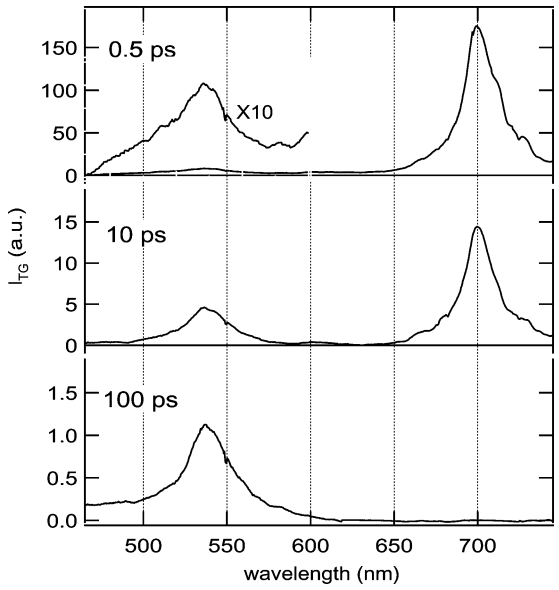

Figure 2. Transient grating spectra recorded at different time delays after the excitation of a solution of Pe with 0.9 M TCNE in ACN.

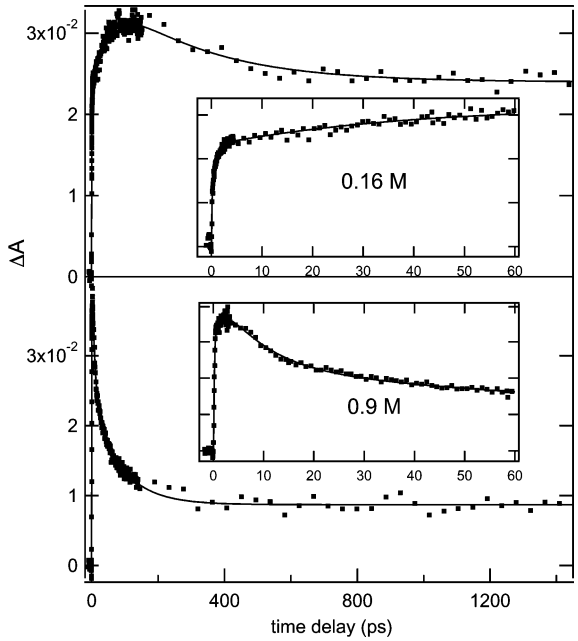

Figure 3. Time profiles of the TA at 535 nm measured with solutions of Pe with different concentrations of TCNE (dots) and best fits of eq 3 (solid line). The insets show a detail of the first 60 ps.

TABLE 2: Parameters Obtained from the Best Fit of Equation 1 to the TA Time Profiles around 535 nm Measured with Various TCNE Molar Concentrations

[TCNE]	A_0	A_1	τ_1 (ps)	A_2	τ_2 (ps)	A_3	τ_3 (ps)
0.16	0.77	0.23	278	−0.45	49	−0.33	1.3
0.32	0.60	0.40	237	0.32	26	−0.56	1.4
0.64	0.39	0.49	132	0.12	5.9	−0.77	1.2
0.9	0.22	0.35	89	0.43	9.2	−0.49	1.9

only the slower component is observed. The time constant associated with this component decreases markedly with increasing TCNE concentration. These dynamic features are associated with the decay of the GIP population upon CR and dissociation.

TABLE 3: Parameters of the Long-Lived Ion Pairs Calculated Using Equations 4 and 5 at Different TCNE Molar Concentrations

[TCNE]	Φ_{ion}[a]	Φ_{ll}[b]	Φ^{ll}_{sep}[c]	k^{ll}_{CR} (ns^{-1})[d]	k^{ll}_{sep} (ns^{-1})[e]
0.008	0.20				
0.03	0.14				
0.06	0.11				
0.16	0.07[f]	0.11	.63	2.6	4.5
0.32	0.06	0.10	.60	2.4	3.5
0.64	0.03[f]	0.06	.50	5.3	5.3
0.9	0.02[f]	0.05	.43	6.3	4.8

[a] Measured free-ion yield, Φ_{ion}, normalized at unit quenching efficiency. [b] Formation efficiency, Φ_{ll}. [c] Separation efficiency, Φ^{ll}_{sep}. [d] CR rate constant, k^{ll}_{CR}. [e] Rate constant of separation, k^{ll}_{sep}. [f] Determined from the height of the plateau in the transient absorption data.

It should be noted that if $I^{S1}_{TA}(t)$ is not subtracted from the TA time profiles, the time constants obtained from the fit remain almost unchanged and the amplitudes do not vary by more than 20%.

Free-Ion Yields. The values of the free-ion yields, Φ_{ion}, corrected to unit quenching efficiency and determined by transient photoconductivity, are listed in Table 3. The free-ion yields at 0.16, 0.64, and 0.9 M were determined from the Φ_{ion} value at 0.32 M and by comparing the relative height of the plateau of the TA profile, A_0 (see Table 2). The free-ion yield of 0.14 measured by Kikuchi and co-workers[30] at [TCNE] = 0.01 M using a different technique compares well with the values found here.

In principle, the free-ion yield can also be obtained from the TA time profile alone (i.e., from the height of the plateau relative to the initial signal intensity extrapolated to $t = 0$). In the present case, this corresponds precisely to the A_0 values listed in Table 2. This is the procedure used in ref 13, where a Φ_{ion} of 0.57 at 0.5 M TCNE was reported. This value agrees quite well with the A_0 found here at similar concentrations. However, such a determination of Φ_{ion} is possible only if the initial signal intensity extrapolated to $t = 0$ accounts for the whole ion population. If this is not the case, then the ion yield will be overestimated. A comparison of Tables 2 and 3 shows that the A_0 values, hence the ion yields obtained from the TA time profiles, are about 10 times larger than the free-ion yields determined by more direct methods. This indicates that the initial TA signal intensity accounts for only 10% of the total ion population. Therefore, although the whole excited Pe population is quenched, as shown by the fluorescence measurements, about 90% of the resulting ion pair population is not visible in the TA data even at very high quencher concentrations!

Discussion

From the data presented above, it is immediately clear that the CR dynamics of the $Pe^{\bullet +}/TCNE^{\bullet -}$ pair is considerably more complex than assumed in previous investigations. Kikuchi and co-workers have estimated the CR rate constant, k_{CR}, from the free-ion yield and the following relationship:[30]

$$\Phi_{ion} = \Phi_q \cdot \Phi_{sep} = \Phi_q \cdot \frac{k_{sep}}{k_{sep} + k_{CR}} \qquad (2)$$

where Φ_q and Φ_{sep} are the quenching and separation efficiencies, respectively, and k_{sep} is the rate constant for the dissociation of the ion pair. Using a k_{sep} value of 1.6×10^9 s^{-1}, these authors obtained a k_{CR} value of 9.8×10^9 s^{-1} at 0.01 M TCNE.

TABLE 4: Parameters Obtained from the Best Fit of Equation 3 to the TA Time Profiles around 535 nm Measured with Various TCNE Molar Concentrations

[TCNE]	A_0	A_1	τ_1 (ps)	A_2	τ_2 (ps)	A_3	τ_3 (ps)
0.16	0.05	0.03	140	0.05	37	0.87	2.4
0.32	0.03	0.02	170	0.06	28	0.89	1.8
0.64	0.02	0.02	94	0.12	5.1	0.84	0.4
0.9	0.02	0.02	90	0.14	5	0.82	0.3

Because of the relatively low time resolution of the measurements performed in the previous TA investigation,[12,13] only the slower decay component of the $Pe^{\bullet+}$ population could be observed. A CR rate constant of $k_{CR} = 6.1 \times 10^8\ s^{-1}$ was obtained by assuming that the rate constant associated with the observed decay is equal to $k_{sep} + k_{CR}$ and from eq 2 with $\Phi_{ion} = 0.57$. Given the low driving force for CR of this ion pair, such a small k_{CR} was interpreted as evidence of the normal region for CR of ion pairs formed by ET quenching.

The above-mentioned investigations assume that all of the ion pairs formed by ET quenching have the same CR dynamics.[12,13,30] The results presented here show that this is not the case. Because of this, the extraction of a single CR rate constant is not possible. The time constants listed in Tables 1 and 2 show that the ET quenching and the Pe cation dynamics are not largely different. Because the ions are formed through the excited Pe population, the contribution of the ion population to the TA profile, $I_{TA}^{ion}(t)$, can be described by the following convolution integral:

$$I_{TA}^{ion}(t) = C \cdot \int_0^t P_{ion}(t - t') \cdot P_{S1}(t')\, dt' \qquad (3)$$

where C is a constant, $P_{S1}(t)$ is the time evolution of the excited Pe population, and $P_{ion}(t)$ is the time evolution of the ion population assuming instantaneous formation at time $t = 0$. If both $P_{S1}(t)$ and $P_{ion}(t)$ exhibit monoexponential dynamics with time constants of τ_{S1} and τ_{ion}, respectively, then $I_{TA}^{ion}(t)$ is biexponential with a rising and a decaying component. If $\tau_{S1} < \tau_{ion}$, then the rise time is equal to τ_{S1}, and the decay time is τ_{ion}. However, if the ions decay faster than they are formed (i.e., if $\tau_{ion} < \tau_{S1}$), then the rise time is equal to τ_{ion}, and the decay time is equal to τ_{S1}. Consequently, one has to be careful when trying to relate the time constants obtained from the triexponential fit of $I_{TA}^{ion}(t)$ and listed in Table 2 to CR time constants. To have a more reliable picture of the CR dynamics of the $Pe^{\bullet+}/TCNE^{\bullet-}$ pair, eq 3 was fitted to the TA profiles measured at different TCNE concentrations. $P_{S1}(t)$ was described by triexponential functions with the parameters listed in Table 1. For $P_{ion}(t)$, a multiexponential function of the form of eq 1 was used. As shown in Figure 3, a good fit to the experimental data could be obtained with $n = 3$. The best-fit parameters are listed in Table 4.

If one compares these parameters with those obtained without the reconvolution with $P_{S1}(t)$ and listed in Table 2, then the following features can be observed:

(1) The slowest decay time, τ_1, is now essentially independent of the quencher concentration. Therefore, the dependence found in Table 2 is most probably due to the relatively slow quenching of Pe* at low TCNE concentrations. It should be noted that at TCNE < 0.5 M the uncertainty of the parameters related to the fast components, namely A_2, A_3, τ_2, and τ_3, is very large. Fixing τ_3 at 0.5 ps results in A_2, A_3, and τ_2 values close to those found at higher concentration.

(2) The height of the plateau, A_0, is now in excellent agreement with the free-ion yields listed in Table 3.

(3) A new decay component with a subpicosecond time constant, τ_3, and a large amplitude, A_3, is required to reproduce the experimental data. Because of this ultrafast component, a large fraction of the ion population decays faster than it is formed and is therefore not visible in the TA time profiles, even at 0.9 M TCNE. This component is most probably responsible for the ultrashort rise observed in the TA time profiles.

For the remainder of this paper, all of the amplitudes and time constants will be taken from Table 4.

One can crudely try to separate the ET quenching product into two groups: (1) ion pairs with slow CR dynamics (long-lived ion pairs) responsible for the large time constant τ_1 and (2) ion pairs with fast CR dynamics (short-lived ion pairs) associated with the shorter time constants. It is reasonable to assume that the free-ion population is essentially generated from the long-lived ion pairs. Indeed, the CR of the short-lived pairs is so fast that separation, which proceeds with a rate constant on the order of $10^9\ s^{-1}$, cannot compete. In this case, the free-ion yield can be expressed as

$$\Phi_{ion} = \Phi_q \cdot \Phi_{ll} \cdot \Phi_{sep}^{ll} = \Phi_q \cdot \Phi_{ll} \cdot \frac{k_{sep}^{ll}}{k_{sep}^{ll} + k_{CR}^{ll}} \qquad (4)$$

where Φ_{ll} is the yield of formation of long-lived ion pairs upon quenching and Φ_{sep}^{ll} is their separation efficiency. The latter can be determined from the relative amplitudes of the slowly decaying component and of the plateau, A_1 and A_0, respectively. Moreover, because $\tau_1^{-1} = k_{sep}^{ll} + k_{CR}^{ll}$, Φ_{sep}^{ll} can also be written as

$$\Phi_{sep}^{ll} = \frac{A_0}{A_0 + A_1} = k_{sep}^{ll} \cdot \tau_1 \qquad (5)$$

The values of Φ_{sep}^{ll}, k_{CR}^{ll}, and k_{sep}^{ll} calculated with eq 5 are listed in Table 3. At the concentrations used here, Φ_q is essentially unity, and thus Φ_{ll} can be simply calculated as $\Phi_{ll} = \{\Phi_{ion}\}/\{\Phi_{sep}^{ll}\}$. Table 3 shows that the so-obtained k_{CR}^{ll} and k_{sep}^{ll} increase with increasing TCNE concentration. A probable reason for this effect is our assumption that the slower CR component is related to ion pairs with the same dynamics. In fact, it is more realistic to consider that this population includes ion pairs with different mutual geometries (distance, orientation) and thus with different CR rate constants and separation efficiencies. In this case, the above assumption leads to an overestimation of k_{sep}^{ll}. Moreover, the so-obtained k_{CR}^{ll} should be considered to be an approximated average value. The increase of k_{CR}^{ll} with quencher concentration indicates that geometries favoring CR are more probable at high TCNE concentration. As discussed in more detail later, the distribution of ion pair geometry is closely connected to the orientation and distance of the neutral reactants during the ET quenching process.

Despite this crude approximation, one can see that the average value of k_{CR}^{ll} is in qualitative agreement with the prediction of Marcus theory for ET in the normal region. However, this value concerns only a small fraction, at most 10%, of the whole ion pair population (see Φ_{ll} in Table 3). Because of the relatively low time resolution of the experiment used in the previous investigation,[12,13] only this slowly decaying population could be observed. For this reason, the Φ_{sep}^{ll} values calculated here are very close to the free-ion yields reported in refs 12 and 13. However, these authors were not aware that only a minor fraction of the ion population had been monitored.

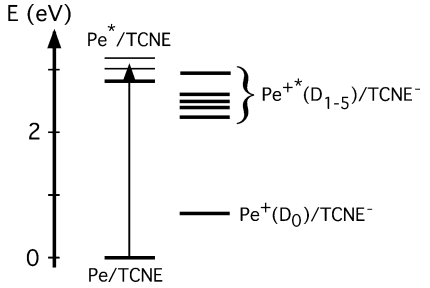

Figure 4. Energy-level diagram for the electron-transfer quenching of Pe by TCNE in ACN.

Most of the ion pair population decays in less than 10 ps. In this case, the direct formation of a CIP upon excitation of a ground-state complex cannot be invoked because this effect is observed even at relatively low TCNE concentration, where no CT band is visible in the absorption spectrum. Moreover, given the time resolution of our experiment, such CIPs would be clearly visible, unless they decay in less than 100 fs. Asahi and Mataga have reported a lifetime of 300 fs for the $Pe^{\bullet+}/TCNE^{\bullet-}$ CIP formed by CT excitation at 710 nm.[15] This lifetime compares very well with the τ_3 time constant found here. Such an ultrafast CR implies that the major product of the ET quenching of Pe* by TCNE is an ion pair with a strong coupling. Indeed, to account for such an ultrashort time constant, an electronic coupling constant larger than about 120 cm^{-1} has to be invoked. Such a large coupling implies that the ions are at contact distance.[31] These strongly coupled ion pairs will thus be called CIPs, although their geometry is probably not so well defined as that of excited donor−acceptor complexes. CIPs are known to be formed upon weakly exergonic ET quenching.[32−35] However, as stated in the Introduction, it has often been suggested that the optimal ET distance for highly exergonic ET is substantially larger than the contact distance (i.e., above 10 Å[5,6,30,36]). If the $Pe^{\bullet+}/TCNE^{\bullet-}$ pairs were formed with a large interionic distance, then the formation of strongly coupled ion pairs would first require some diffusion of the ions.[37,38] However, the lifetime of the ion pairs is too small to allow a significant change in mutual geometry to take place. Consequently, the ultrafast CR dynamics found here is totally incompatible with long-distance ET quenching.

The ultrafast CR dynamics and the driving-force-dependent ET distance model can be reconciled if the electronic excited states of $Pe^{\bullet+}$ are considered. The energy-level diagram shown in Figure 4 indicates that the four lowest excited electronic states of $Pe^{\bullet+}$ are energetically accessible upon ET quenching of Pe* by TCNE.[39] In this case, the driving force for CS ranges from −0.64 to −0.27 eV, and CS at contact distance should thus be optimal. Therefore, the CIPs (i.e., the ion pair population that undergoes ultrafast CR) could be formed in an electronic excited state.

There is, however, no spectroscopic evidence for the formation of such an excited $Pe^{\bullet+}*/TCNE^{\bullet-}$ product. Transient grating spectra measured after the excitation of $Pe^{\bullet+}$ at 532 nm in sulfuric acid indicate that $Pe^{\bullet+}*$ does not absorb significantly between 470 and 750 nm.[40] Therefore, the fact that the spectra shown in Figure 2 contain bands associated only with Pe* and $Pe^{\bullet+}$ does not prove that the primary ET quenching product is the ground-state ion pair.

A strong indication for the formation of an excited quenching product would be a delayed formation of the ground-state ion pair population compared to the decay of Pe*. Such a delayed formation could only be clearly detected if the excited-state lifetime of the CIP were longer than the decay time of the Pe* population. The ground-state recovery time of $Pe^{\bullet+}$ in acetonitrile after excitation in the D_0-D_5 transition has been reported to be shorter than 15 ps.[41] Preliminary measurements with a better time resolution indicate a ground-state recovery time on the order of 3 ps. In principle, the excited CIP could also decay upon CR to the neutral ground state. However, this process is probably too exergonic ($\Delta G_{CR} \approx -2.2$ eV) to compete significantly with internal conversion to the ground-state CIP. Therefore, a 3-ps excited-state lifetime of the CIP is too small compared to the ET quenching dynamics of Pe* to affect significantly the time profile of the ion pair population even at 0.9 M.

We have recently shown that for ion pairs formed upon ET quenching of molecules in the S_2 state, the main CR pathway was the less exergonic one (i.e., that leading to the formation of a product in the electronic excited state[16,42]). In principle, there is no evident reason that this should not also be the case for a charge separation process such as that investigated here.

However, the long-lived ion pair population may be formed directly in the electronic ground state by long-distance CS. Table 3 shows that the formation efficiency of the long-lived ion pairs as well as the free-ion yield depend markedly on the TCNE concentration. This effect could be explained as follows. At low concentration, the probability for an excited Pe molecule to have a quencher molecule at contact distance is relatively small, and thus the ET quenching requires the diffusion of the reactants. Because CS to the ground-state product is highly exergonic, it could occur before the reactants have found a mutual geometry

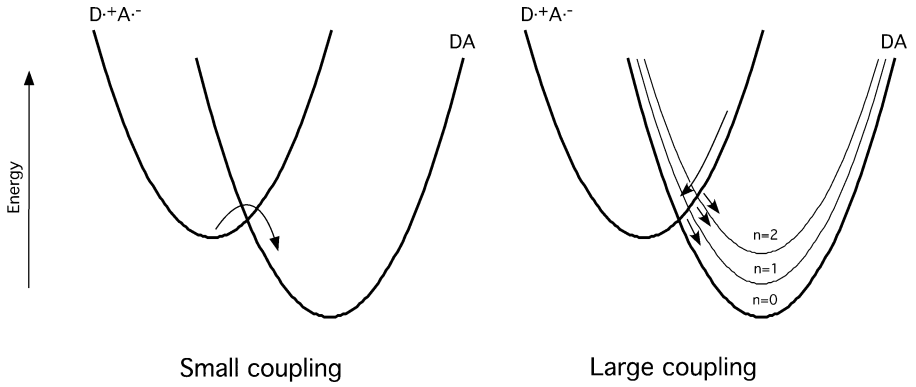

Figure 5. Schematic illustration of the difference in CR dynamics for weakly and strongly coupled ion pairs using cuts in the free-energy surfaces of reactant and product states along a slow coordinate. For weak coupling, CR is much slower than relaxation and is thus thermally activated. For strong coupling, CR is ultrafast and occurs before the relaxation of the ion pair to the equilibrium. The thin parabolas correspond to vibrationally excited states of the product.

or distance with a large coupling constant. The ensuing product can be called an LIP (i.e., an ion pair with an interionic distance larger than that associated with a CIP and with a much smaller electronic coupling constant). Given the larger exergonicity of CS, this ion pair should be formed with a large excess energy. However, because of the small coupling constant, the probability of CR during relaxation to the equilibrium is negligibly small. Once the ion pair has relaxed, CR is a thermally activated process as shown in Figure 5. Therefore, CR is not ultrafast, and the separation into free ions is a competitive process. This is the normal regime predicted by Marcus theory for weakly exergonic nonadiabatic ET processes.

At high quencher concentration, the probability for an excited Pe molecule to have a TCNE molecule at contact distance is large, as reflected by the strong transient effect in the fluorescence decay. In this case, the quenching results mainly in ion pairs with strong coupling, CIPs, either in an excited state or in the ground state. In both cases, the ground-state CIP is populated far from equilibrium. Because of the large electronic coupling, the probability of CR during relaxation is very high (see Figure 5). Consequently, CR is ultrafast, and the free-ion yield is essentially zero. In this case, the nonadiabatic picture no longer really holds because of the large electronic coupling. We have recently shown that nonequilibrium CR dynamics can account for the absence of the normal region observed with excited donor−acceptor complexes.[18] Marcus theory is not suited to treat such a situation where the electronic coupling is very large and where nonequilibrium ET can occur. Consequently, the absence of the normal region for such processes should not be a surprise.

Concluding Remarks

This investigation shows that the charge recombination dynamics of the ion pairs formed upon the highly exergonic electron-transfer quenching of Pe by TCNE is more complex than previously thought. If the measurements are not performed with a sufficiently high time resolution, then only the slower part of the dynamics, which is related to a minor fraction of the ion pair population, is observed. Charge recombination of this small subpopulation is slow, in agreement with Marcus theory for the normal regime. However, the major fraction of the ion pair population does not exhibit the normal behavior. This is due to the fact that more than 90% of the quenching products are strongly coupled ion pairs, even at relatively small quencher concentration.

The determination of the rate constant of charge recombination, k_{CR}, from the free-ion yield is possible only if all of the ion pairs have similar charge recombination dynamics, which is not the case here. Therefore, the observations of the normal region reported so far from an indirect determination of k_{CR} should be considered with caution.

For the system investigated here, long-distance charge separation, if operative, is a minor quenching pathway. Therefore, it cannot account for the absence of the inverted region for highly exergonic bimolecular ET. Consequently, the formation of the quenching product in an electronic excited state remains the most probable hypothesis. However, because of their short lifetime and their lack of spectral features in the visible region, these excited products are very difficult to observe. Further investigations of similar systems are in progress.

Acknowledgment. This work was supported by the Fonds National Suisse de la Recherche Scientifique through project no. 200020-100014.

References and Notes

(1) Weller, A. *Pure Appl. Chem.* **1982**, *54*, 1885.
(2) Marcus, R. A.; Sutin, N. *Biochim. Biophys. Acta* **1985**, *811*, 265.
(3) Rehm, D.; Weller, A. *Isr. J. Chem.* **1970**, *8*, 259.
(4) Brunschwig, B. S.; Ehrenson, S.; Sutin, N. *J. Am. Chem. Soc.* **1984**, *106*, 6858.
(5) Kakitani, T.; Matsuda, N.; Yoshimori, A.; Mataga, N. *Prog. React. Kinet.* **1995**, *20*, 347.
(6) Murata, S.; Tachiya, M. *J. Phys. Chem.* **1996**, *100*, 4064.
(7) Mataga, N.; Asahi, T.; Kanda, Y.; Okada, T.; Kakitani, T. *Chem. Phys.* **1988**, *127*, 249.
(8) Levin, P. P.; Pluzhnikov, P. F.; Kuzmin, V. A. *Chem. Phys. Lett.* **1988**, *147*, 283.
(9) Suppan, P. *Top. Curr. Chem.* **1992**, *163*, 95.
(10) Vauthey, E. *J. Phys. Chem. A* **2001**, *105*, 340.
(11) Asahi, T.; Mataga, N. *J. Phys. Chem.* **1989**, *93*, 6575.
(12) Mataga, N.; Kanda, Y.; Okada, T. *J. Phys. Chem.* **1986**, *90*, 3880.
(13) Mataga, N.; Kanda, Y.; Asahi, T.; Miyasaka, H.; Okada, T.; Kakitani, T. *Chem. Phys.* **1988**, *127*, 239.
(14) Gould, I. R.; Young, R. H.; Moody, R. E.; Farid, S. *J. Phys. Chem.* **1991**, *95*, 2068.
(15) Asahi, T.; Mataga, N. *J. Phys. Chem.* **1991**, *95*, 1956.
(16) Morandeira, A.; Engeli, L.; Vauthey, E. *J. Phys. Chem. A* **2002**, *106*, 4833.
(17) Nicolet, O.; Vauthey, E. *J. Phys. Chem. A* **2003**, *107*, 5894.
(18) Nicolet, O.; Vauthey, E. *J. Phys. Chem. A* **2002**, *106*, 5553.
(19) Vauthey, E.; Pilloud, D.; Haselbach, E.; Suppan, P.; Jacques, P. *Chem. Phys. Lett.* **1993**, *215*, 264.
(20) von Raumer, M.; Suppan, P.; Jacques, P. *J. Photochem. Photobiol., A* **1997**, *105*, 21.
(21) Henseler, A.; Vauthey, E. *J. Photochem. Photobiol., A* **1995**, *91*, 7.
(22) Morandeira, A.; Furstenberg, A.; Gumy, J.-C.; Vauthey, E. *J. Phys. Chem. A* **2003**, *107*, 5375.
(23) Pigliucci, A.; Vauthey, E. *Chimia* **2003**, *57*, 200.
(24) Hochstrasser, R. M.; Nyi, C. *J. Chem. Phys.* **1980**, *72*, 2591.
(25) Rice, S. A. *Diffusion-Limited Reactions*; Comprehensive Chemical Kinetics; Elsevier: New York, 1985; Vol. 25.
(26) Högemann, C.; Pauchard, M.; Vauthey, E. *Rev. Sci. Instrum.* **1996**, *67*, 3449.
(27) Högemann, C.; Vauthey, E. *Isr. J. Chem.* **1998**, *38*, 181.
(28) Shida, T. *Electronic Absorption Spectra of Radical Ions*; Physical Sciences Data; Elsevier: Amsterdam, 1988; Vol. 34.
(29) Fayer, M. D. *Annu. Rev. Phys. Chem.* **1982**, *33*, 63.
(30) Kikuchi, K.; Niwa, T.; Takahashi, Y.; Ikeda, H.; Miyashi, T. *J. Phys. Chem.* **1993**, *97*, 5070.
(31) Castner, E. W., Jr.; Kennedy, D.; Cave, R. J. *J. Phys. Chem. A* **2000**, *104*, 2869.
(32) Gould, I. R.; Young, R. H.; Mueller, L. J.; Farid, S. *J. Am. Chem. Soc.* **1994**, *116*, 8176.
(33) Vauthey, E.; Högemann, C.; Allonas, X. *J. Phys. Chem. A* **1998**, *102*, 7362.
(34) Kikuchi, K.; Niwa, T.; Takahashi, Y.; Ikeda, H.; Miyashi, T.; Hoshi, M. *Chem. Phys. Lett.* **1990**, *173*, 421.
(35) Kuzmin, M. G.; Sadovskii, N. A.; Weinstein, J.; Kutsenok, O. *Proc. − Indian Acad. Sci., Chem. Sci.* **1993**, *105*, 637.
(36) Jacques, P.; Allonas, X. *Chem. Phys. Lett.* **1995**, *233*, 533.
(37) Burshtein, A. I.; Shokhirev, N. V. *J. Phys. Chem. A* **1997**, *101*, 25.
(38) Burshtein, A. I. *Adv. Chem. Phys.* **2000**, *114*, 419.
(39) Hirata, S.; Lee, T. J.; Head-Gordon, M. *J. Chem. Phys.* **1999**, *111*, 8904.
(40) Brodard, P.; Sarbach, A.; Gumy, J.-C.; Bally, T.; Vauthey, E. *J. Phys. Chem. A* **2001**, *105*, 6594.
(41) Gumy, J.-C.; Vauthey, E. *J. Phys. Chem. A* **1997**, *101*, 8575.
(42) Muller, P.-A.; Vauthey, E. *J. Phys. Chem. A* **2001**, *105*, 5994.